Neuroscience 275 (2014) 125–135

GENERATION OF INDUCED NEURONS BY DIRECT REPROGRAMMING IN THE MAMMALIAN COCHLEA

K. NISHIMURA, [a*†] **R. M. WEICHERT,** [b†] **W. LIU,** [c†] **R. L. DAVIS** [c] **AND A. DABDOUB** [a,d,e*]

[a] *Biological Sciences, Sunnybrook Research Institute, 2075 Bayview Avenue, Toronto, ON M4N 3M5, Canada*

[b] *Department of Surgery/Otolaryngology, UCSD School of Medicine, La Jolla, CA 92093, USA*

[c] *Department of Cell Biology and Neuroscience, Nelson Laboratories, Rutgers University, 604 Allison Road, Piscataway, NJ 08854, USA*

[d] *Department of Otolaryngology – Head and Neck Surgery, University of Toronto, Toronto, ON, Canada*

[e] *Department of Laboratory Medicine and Pathobiology, University of Toronto, Toronto, ON, Canada*

Abstract—Primary auditory neurons (ANs) in the mammalian cochlea play a critical role in hearing as they transmit auditory information in the form of electrical signals from mechanosensory cochlear hair cells in the inner ear to the brainstem. Their progressive degeneration is associated with disease conditions, excessive noise exposure and aging. Replacement of ANs, which lack the ability to regenerate spontaneously, would have a significant impact on research and advancement in cochlear implants in addition to the amelioration of hearing impairment. The aim of this study was to induce a neuronal phenotype in endogenous non-neural cells in the cochlea, which is the essential organ of hearing. Overexpression of a neurogenic basic helix–loop–helix transcription factor, *Ascl1*, in the cochlear non-sensory epithelial cells induced neurons at high efficiency at embryonic, postnatal and juvenile stages. Moreover, induced neurons showed typical properties of neuron morphology, gene expression and electrophysiology. Our data indicate that *Ascl1* alone or *Ascl1* and *NeuroD1* is sufficient to reprogram cochlear non-sensory epithelial cells into functional neurons. Generation of neurons from non-neural cells in the cochlea is an important step for the regeneration of ANs in the mature mammalian cochlea.

Key words: reprogramming, auditory neurons, cochlear non-sensory epithelial cells, regeneration, spiral ganglion, hearing.

INTRODUCTION

The potential of transcription factors in inducing somatic cells into differentiated cells has been known since the demonstration of *MyoD*'s capability to transform fibroblasts into muscle-like cells (Davis et al., 1987). More recent work has proven that transcription factors can help shuttle between differentiated cells: pancreatic exocrine cells derive from pancreatic endoderm, as do β-cells (Gu et al., 2002), and the basic helix–loop–helix (bHLH) transcription factor *neurogenin3*, in combination with *Pdx1* and *Mafa*, can efficiently convert pancreatic exocrine cells into β-cells *in vivo* (Zhou et al., 2008). Previously, using the transcription factors *neurogenin1* (*Neurog1*), *NeuroD1* and *SRY-related high-mobility-group box 2* (*Sox2*), we demonstrated that cochlear non-sensory epithelial cells were competent to develop as neurons as ectopic expression of these factors was sufficient to induce a neuronal phenotype (Puligilla et al., 2010). However, neuronal induction of non-sensory cells only occurred at embryonic stages, and even then the efficiency of induction was relatively low.

Cochlear non-sensory epithelial cells, mechanosensory hair cells, their supporting cells and auditory neurons (ANs) develop from the otic placode (Rubel and Fritzsch, 2002). Cochlear hair cells are innervated by the bipolar ANs, which are responsible for conveying auditory signals from hair cells to the brain. Loss of auditory hair cells or ANs in the inner ear is the leading cause of congenital and acquired hearing impairment (Rubel and Fritzsch, 2002). For patients who do not have residual hearing, a cochlear implant, which directly stimulates ANs electrically, has been the only solution to restore their hearing. So far, no biological therapy to treat sensorineural hearing loss has been available mainly due to the lack of regeneration capacity in the adult inner ear. While the loss of ANs has been considered secondary to hair cell loss, an increasing body of evidence clearly indicates that ANs can degenerate as a result of noise exposure and aging while hair cells remain intact (Kujawa and Liberman, 2009; Lin et al., 2011; Engle et al., 2013;

*Corresponding authors. Address: Sunnybrook Research Institute, 2075 Bayview Avenue, Toronto, ON M4N 3M5, Canada. Tel: +1-4164806100; fax: +1-4164804375 (A. Dabdoub).
E-mail addresses: knishimu@sri.utoronto.ca (K. Nishimura), rmacki08@yahoo.com (R. M. Weichert), wenkeliu@rutgers.edu (W. Liu), rldavis@dls.rutgers.edu (R. L. Davis), alain.dabdoub@sri.utoronto.ca (A. Dabdoub).
† These authors contributed equally.

Abbreviations: ANs, auditory neurons; bHLH, basic helix–loop–helix; DIV, days *in vitro*; EDTA, ethylenediaminetetraacetic acid; EGTA, ethylene glycol tetraacetic acid; FBS, fetal bovine serum; GER, greater epithelial ridge; HBSS, Hank's balanced salt solution; HEPES, 4-(2-hydroxyethyl)piperazine-1-ethanesulfonic acid; LER, lesser epithelial ridge; Map2, microtubule-associated protein 2; SE, sensory epithelium; SNAP25, synaptosomal-associated protein-25; Sox2, SRY-related high-mobility-group box 2; TTX, tetradotoxin.

http://dx.doi.org/10.1016/j.neuroscience.2014.05.067
0306-4522/

Furman et al., 2013; Sergeyenko et al., 2013). Age-related primary degeneration of ANs in human temporal bones may contribute to the decline in hearing-in-noise performance (Makary et al., 2011). Moreover, several genetic mutations result in primary loss of ANs: a mutation in mitochondrial DNA, most commonly an A→G mutation at locus 3243, causes degenerative changes in ANs while the organ of Corti is generally spared (Nadol and Merchant, 2001; Takahashi et al., 2003), and mutations in the TIMM8A gene, which causes mitochondrial dysfunction, cause primary degeneration of ANs with the majority of the organ of Corti remaining intact (Bahmad et al., 2007). Therefore, inducing the regeneration of ANs in a damaged ear has significant implications for future advances in the biological treatment of deafness.

Recently, combinatorial expression of neural-lineage-specific transcription factors, including the bHLH transcription factor *Ascl1* (*Mash1*), was shown to directly convert embryonic and postnatal fibroblasts into neurons (Vierbuchen et al., 2010; Pang et al., 2011). Furthermore, *Ascl1* alone was sufficient to induce neurons from mouse fibroblasts (Vierbuchen et al., 2010), and *Ascl1* was directly linked to the expansion of neural progenitors, later cell cycle exit and neural differentiation (Castro et al., 2011). Based on these findings and the need to induce neurons at high efficiency in postnatal and adult inner ears, we investigated the neurogenic transcription factor, *Ascl1*, to examine its ability to directly convert embryonic and postnatal cochlear non-sensory epithelial cells into neurons. We show that *in vitro* overexpression of *Ascl1* in the non-sensory epithelial cells of both embryonic and postnatal mouse cochlea is sufficient to generate induced neurons at high efficiency, as defined by morphology, expression of neuronal markers, synaptic proteins and the generation of action potentials.

EXPERIMENTAL PROCEDURES

Experimental animals

Pregnant CD-1 and CBA/CaJ mice were obtained from the Charles River Laboratories. Embryonic day 13.5 (E13.5) and postnatal day (P1, 5, 10 and 20) mice were used to perform gain-of-function experiments, immunohistochemistry and electrophysiological recordings. All procedures involving animals were approved by the Sunnybrook Research Institute Animal Care and Use Committee, being conformed to the guidelines set out by the Canadian Council on Animal Care, the University of California San Diego Institutional Animal Care and Use Committee, and the Rutgers University Institutional Review Board for the Use and Care of Animals.

DNA constructs

The *pCIG.nucEGFP.Ascl1* expression vector and the control *pCIG.nucEGFP* vector were kindly provided by S. Pons (Institute for Biomedical Research of Barcelona) (Alvarez-Rodriguez and Pons, 2009). A *pCLIG-NeuroD1* expression vector was kindly provided by R. Kageyama (Kyoto University, Kyoto, Japan) (Inoue et al., 2002). The pCLIG vector uses a *CMV-IE enhancer/chicken β-actin promoter* and an *Internal Ribosomal Entry Site* (*IRES*) to drive the expression of *NeuroD1* and *EGFP* as independent transcripts. The *pCIG.nucEGFP* vector and the *cytoplasmic.RFP* vector (Clontech) were used as control vectors.

Electroporation of cochlear explant cultures

Cochlear explants were dissected at E13.5, P1, P5, P10 and P20. Cochlear explants at E13.5, P1 and P5 were electroporated as described previously (Jones et al., 2006; Dabdoub et al., 2008). In brief, the cochlear disk was oriented perpendicular to the surface of the Petri dish in a 10-μl drop of PBS containing 1-μg/μl DNA of the specific expression vector(s) or a control vector. The two electrodes were placed on opposite sides of the disk and the negative electrode was located facing the luminal surface of the sensory epithelium (SE) (Fig. 1A). For cells to be transfected with multiple expression vectors, equal concentrations of the desired expression plasmids (1.0-μg/μl for each vector) were electroporated (Fig. 1E) (Ono et al., 2009; Masuda et al., 2012). A ECM830 square wave electroporator (BTX Harvard Apparatus, Holliston, MA, USA) was used for electroporation. The following parameters were used: 27 V, 30-ms duration, 100-ms interval, 9 pulses per cochlea. For electroporation of P10 and P20 cochlear explants, the apical portion of the cochlea was used. The cochlear disk was placed in an electroporation chamber with a 2-mm^2 electrode surrounded by a silicone rubber sheet, and a 10-μl drop of PBS containing 1-μg/μl DNA was applied in the chamber and the negative electrode was located facing to the luminal surface of the SE (Fig. 1B). The following parameters were used: 14 V, 30-ms duration, 100-ms interval, 8 pulses per cochlea. As soon as pulsing was finished, 50 μl of culture media was immediately added to the droplet. Following electroporation, cochleae were established as explants with the luminal surface of the SE facing upward on MatTek dishes (MatTek Corporation, Ashland, MA, USA) coated with a layer of Matrigel (1:20 dilution; BD Biosciences, San Jose, CA, USA). Explants were maintained at 35 °C for at least 6 days *in vitro* (DIV) in 150 μl of culture media with 10% fetal bovine serum (FBS) and processed by immunohistochemistry.

Immunohistochemistry

Cochleae from embryos and newborn pups were removed, isolated, and processed as whole mounts. Immunocytochemistry was performed on cochlear explant cultures as described previously (Dabdoub et al., 2008; Puligilla et al., 2010). Cells were labeled with primary antibodies against TuJ1 (1:500; Sigma, St.Louis, MO, USA), microtubule-associated-protein 2 (Map2; 1:300; Sigma, St.Louis, MO, USA), Prox1 (1:250; R&D Systems, Minneapolis, MN, USA), synaptosomal-associated protein-25 (SNAP25; 1:1000; Covance, Berkeley, CA, USA), Synapsin I (1:1000; Millipore, Billerica, MA, USA), Myosin 7a (1:100; Developmental Hybridoma Bank, Iowa City, IA, USA) Sox2 (1:250; Santa Cruz Biotechnology, Dallas, TX, USA), Myosin 6 (1:1000; Proteus

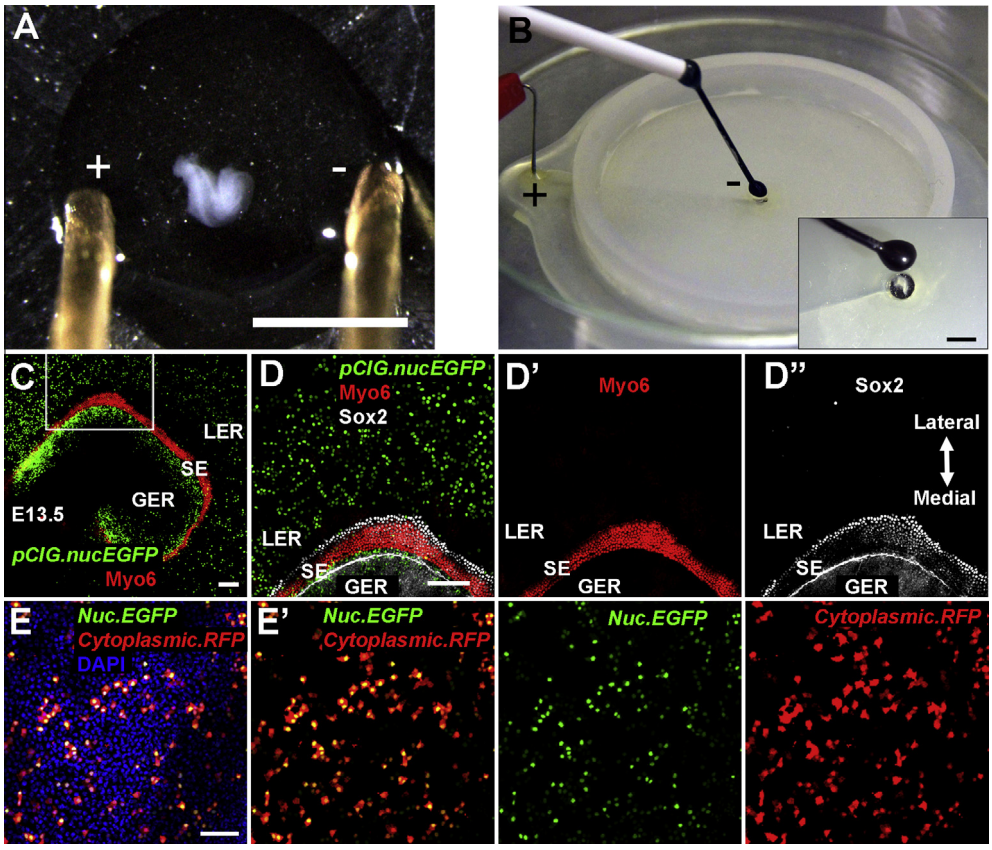

Fig. 1. Plasmid DNA is electroporated in the cochlear epithelial cells at embryonic, postnatal and juvenile stages. (A) Procedures of electroporation at E13.5, P1 and P5. The negative electrode was located facing the lumenal surface of the sensory epithelium, while the positive electrode faced the mesenchyme. (B) Procedures of electroporation at P10 and P20. The apical portion of the cochlea at P10 and P20 is positioned so that the negative electrode is facing the sensory epithelium. Inset, high-magnification view of the electrodes and the cochlea. (C) Low-magnification image of an E13.5 cochlear explant culture electroporated with *pCIG.nucEGFP* control vector (green) and maintained for 6 DIV. Sensory epithelium (SE) is indicated by Myosin 6-positive cochlear hair cells (red). Non-sensory epithelial cells in the LER are lateral to SE and those in the GER are medial to SE. D, High-magnification image of C, in addition of Sox2-positive supporting cells (white). (D') Only Myosin 6-positive cells (red) are indicated. (D'') only Sox2-positive supporting cells are indicated. Transfection of cells with multiple expression vectors was achieved by electroporation with equal concentration of the desired expression vectors. Non-sensory cells in the LER of E13.5 were doubly transfected with *pCIG.nucEGFP* (green) and *cytoplasmic.RFP* (red). (E) Merged view of GFP (green) and RFP (red) counterstained with DAPI (blue). (E') The same view as in E, except without DAPI. Individual channels are shown to the right. Scale bar: A and B, 2 mm; C–E, 100 μm. (For interpretation of the references to color in this figure legend, the reader is referred to the web version of this article.)

Biosciences, Ramona, CA, USA) and 4′,6-diamino-2-phenylindole (DAPI) (1:3000; Roche, Penzberg, Upper Bavaria, Germany). SE includes Myosin 6-positive cochlear hair cells (Fig. 1C, D, D') and Sox2-positive supporting cells (Fig. 1D, D''). Non-sensory epithelial cells in the greater epithelial ridge (GER) are lateral to SE, whereas those in the lesser epithelial ridge (LER) are medial to SE (Fig. 1D–D'').

Electrophysiology

Just after electroporation, cochlear explants were digested with 0.25% Trypsin–EDTA in Hank's balanced salt solution (HBSS) (Cellgro Medical Tech, Manassas, VA, USA) at 37 °C for 10 min. The trypsinization was stopped by the addition of FBS, and the tissue was triturated by pipetting up and down 20–30 times gently. The dissociated cells were then plated. Recordings were made with glass pipettes (Sutter Instruments, Novato, CA, USA, cat.# BF 150-110-10) pulled on a vertical puller (Narishige, Setagaya-ku, Tokyo, Japan, model# PP-83) and coated with Sylgard (Dow Corning, Midland, MI, USA). Immediately before use, pipette tips were fire-polished, and pipettes with resistance ranging from 3 to 10 MΩ were used. Experiments were performed at room temperature and pipette offset currents were zeroed just before contacting the cell surface. Recordings were made with Axopatch 200A amplifier (Axon Instruments, Union, CA, USA) and I_{fast} circuitry was used for whole-cell current clamp mode. Data were digitized at 5 kHz and filtered at 1 kHz. Programs of data acquisition and analysis were generously contributed by Dr. Mark Plummer, Rutgers University. Pipettes were filled with internal solution as follows: 112 mM KCl, 0.1 mM $CaCl_2$, 2 mM $MgCl_2$, 11 mM ethylene glycol tetraacetic acid (EGTA), 10 mM 4-(2-hydroxyethyl)piperazine-1-ethanesulfonic acid (HEPES), pH 7.5. Cells were exposed to bath solution: 136.9 mM NaCl, 5.4 mM KCl, 1.67 mM $CaCl_2$, 0.98 mM $MgCl_2$, 16.7 mM glucose, 50 mM sucrose, 10 mM HEPES, pH 7.5, 330 mOsm. For tetradotoxin (TTX) blocking experiments, TTX was prepared as 1 mM stock solution

and was diluted in bath solution to the final concentration of 1 μM before use. Leak-subtraction was applied to all whole-cell voltage clamp traces before measurements.

Data analysis

Cells were counted in a minimum of three different explant cultures from at least two different litters. Transfected cells were counted at random based on expression of the GFP marker. A neuronal cell fate was then determined based on expression of neuronal marker TuJ1 (βIII-tubulin) (Lee et al., 1990; Hallworth et al., 2000). In order to keep the count unbiased cells were picked by screening for green (GFP) at first, followed by calculation of the ratio for the expression of TuJ1 in GFP-positive cells. The average value for each explant was used in the analysis. All data are presented as the mean ± standard error of the mean (SEM). Total number of explants (*e*) and transfected cells (*t*) is also presented. Statistical differences between the two groups were assessed with one-tailed Student's *t* test. P values of less than 0.05 were considered to be significant.

RESULTS

Direct conversion of cochlear non-sensory cells to neurons by *Ascl1*

The role of *Ascl1* as an efficient neural reprograming gene led us to investigate whether *Ascl1* suffices to induce neuronal identity in non-sensory cochlear epithelial cells. To test this hypothesis, electroporation-mediated gene transfection was used to overexpress *Ascl1*. While cells in both the GER and LER were transfected (Figs. 1C, D and 2A), only transfected cells in the LER were evaluated at E13.5, P1, P5 and P10 as endogenous neurons reside in the GER. At P20, we were able to electroporate cells in the sensory domain only; therefore we evaluated cells in the sensory region at P20 and compared them to prosensory cells at E13.5. After 6–7 DIV, development of neuronal phenotypes was evaluated based on morphology and expression of the neuronal markers TuJ1 (βIII-tubulin) (Lee et al., 1990; Hallworth et al., 2000), Map2 (Hafidi et al., 1992) and Prox1 (Bermingham-McDonogh et al., 2006; Karalay et al., 2011).

The majority of non-sensory epithelial cells at E13.5 transfected with *Ascl1* were positive for TuJ1 (Fig. 2A-D; Fig. 3C). Ascl1-transfected cells with neural morphologies were also positive for Map2 (Fig. 2C) and Prox1 (Fig. 2D). Moreover, transfected cells at P1, P5, P10 and P20 were positive for TuJ1, extending long processes (Fig. 3A, A', B). In contrast, untransfected cells (Figs. 2B, C and 3A) and cells transfected with the control *pCIG.nucEGFP* vector (Fig. 3C, D; data not shown) were consistently negative for TuJ1, indicating the specificity of neuron induction.

To determine the efficiency of neuron induction at different embryonic and postnatal stages, the percentage of *Ascl1.pCIG.nucEGFP*-transfected cells that expressed TuJ1 was determined (Fig. 3C, D). *Ascl1* induced non-sensory epithelial cells into neuronal cells at high efficiency both at embryonic and postnatal stages. As shown in Fig. 3C, 91 ± 2% of cells transfected with *Ascl1.EGFP* at E13.5 ($e = 4$, $t = 327$) were positive for TuJ1. 75 ± 7% of cells were positive for TuJ1 at P1 ($e = 4$, $t = 248$), 76 ± 7% at P5 ($e = 12$, $t = 204$) and 73 ± 8% at P10 ($e = 19$, $t = 201$). Additionally, *Ascl1* induced sensory epithelial cells into neuronal cells both at embryonic and juvenile stages. As shown in Fig. 3D, 77 ± 7% of cells at E13.5 ($e = 4$, $t = 538$) and 43 ± 7% of cells at P20 ($e = 25$, $t = 166$) were positive for TuJ1. All of non-sensory epithelial cells ($e = 3$, $t = 197$) and sensory epithelial cells ($e = 5$, $t = 228$) at E13.5 transfected with the control *pCIG.nucEGFP* vector were negative for TuJ1.

We examined the expression of Synapsin I, which is present in the nerve terminal of axons and is an important regulator of the reserve pool of synaptic vesicles (De Camilli et al., 1983; Shupliakov et al., 2011) and is present in the ANs *in vitro* (Martinez-Monedero et al., 2006). We also examined the expression of SNAP25, which is a component of the soluble *N*-ethyl-maleimide-sensitive factor attachment receptor complex responsible for synaptic vesicle exocytosis (Rizo and Sudhof, 2002; Flores-Otero et al., 2007), and is enriched in apical ANs (Flores-Otero et al., 2007). Ascl1-transfected non-sensory epithelial cells expressed Synapsin I and SNAP25 (data not shown).

Here we have shown that ectopic expression of *Ascl1* is sufficient to induce functional neurons in non-sensory epithelial cells in the LER at embryonic and postnatal stages. However, mere expression of neuronal protein is not enough to define functional ANs, prompting us to make use of the bHLH transcription factor *NeuroD1*, which regulates differentiation of ANs during development (Kim et al., 2001). NeuroD1-transfected cells were positive for TuJ1 as well as positive for Synapsin I and SNAP25 (data not shown), agreeing with the previous report (Puligilla et al., 2010). In order to further induce AN-specific neuron development, a combination of *Ascl1* and *NeuroD1* were doubly overexpressed in cochlear non-sensory epithelial cells. Transfection of cells with multiple expression vectors is achieved by electroporation with equal concentrations of the desired expression vectors (Fig. 1E, E'). Cells that were doubly transfected with *Ascl1.nucEFGP* and *NeuroD1.EGFP* with neural morphologies expressed SNAP25 (Fig. 4A) and Synapsin I (Fig. 4B). We did not observe any difference regarding expression and distribution of synaptic proteins between single and double transfection.

Ascl1-induced neurons are functional

The intrinsic firing features of ANs have been well characterized in postnatal *in vitro* cultures. ANs exhibit tonotopic variation as well as local heterogeneity of firing features such as accommodation, voltage threshold and action potential latency (Adamson et al., 2002; Liu and Davis, 2007). Overall, as demonstrated by short latency and brief duration of action potentials, the majority of postnatal ANs are capable of very rapid response to depolarization.

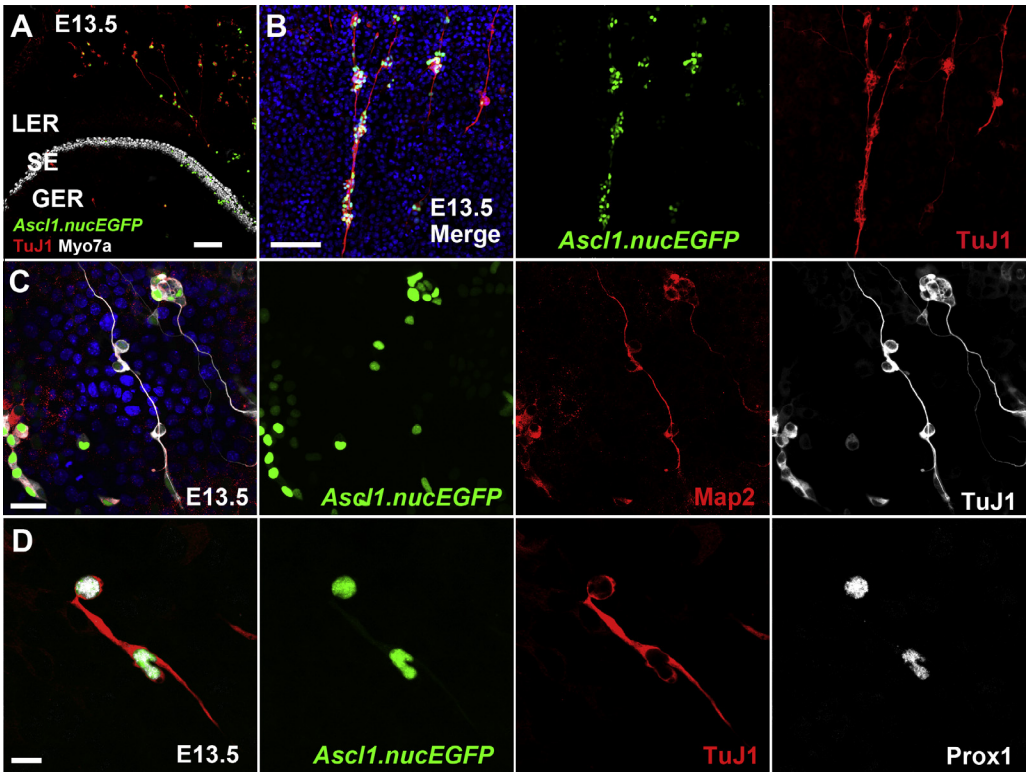

Fig. 2. Neurons are induced quickly and efficiently by Ascl1. Low- (A) and high- (B–D) magnification images of E13.5 cochlear explant cultures electroporated with *Ascl1.nucEGFP* and maintained for 6 DIV. Low-magnification image (A) shows sensory epithelium (SE) and nonsensory epithelium including GER and LER. SE includes cochlear hair cells, which are Myo7a-positive (A in white). Merged views are shown on the left (B, C, D) and individual channels are to the right. Cochlear non-sensory epithelial cells transfected with *Ascl1.nucEGFP* (green) express TuJ1 (A,B,D in red; C in white), Map2 (C in red) and Prox1 (D in white) and display complex neuronal morphologies. Scale bar: A and B, 100 μm; C, 30 μm; D, 10 μm. (For interpretation of the references to color in this figure legend, the reader is referred to the web version of this article.)

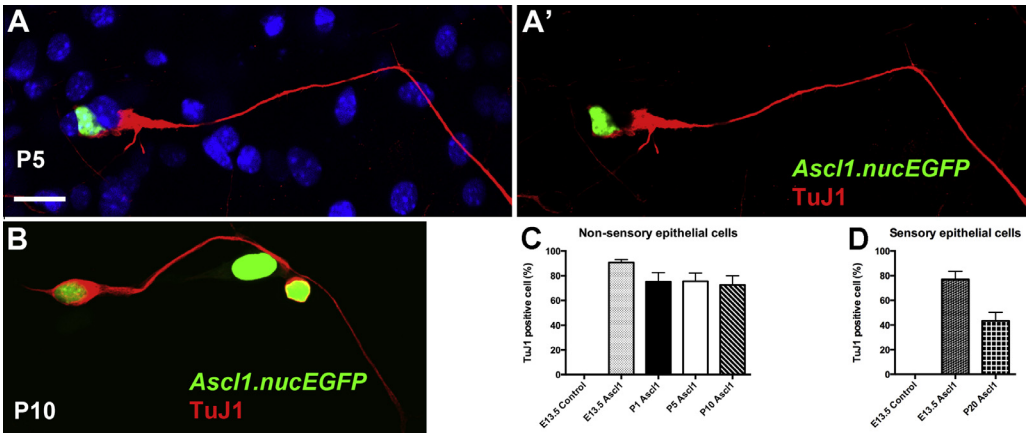

Fig. 3. Ascl1-induced neurons at postnatal and juvenile stages. (A) High-magnification image of P5 cochlear nonsensory epithelial cells in the LER electroporated with *Ascl.nucEGFP* (green) and maintained for 7 DIV immunostained for TuJ1 (red) and counterstained against DAPI (blue). A', The same image as in A, except without DAPI. (B) High-magnification image of P10 cochlear nonsensory epithelial cells electroporated with *Ascl.nucEGFP* (green) and maintained for 7 DIV immunostained for TuJ1 (red). (C) High-magnification image of E13.5 cochlear nonsensory epithelial cells electroporated with *Ascl.nucEGFP* (green) and maintained for 7 DIV immunostained for TuJ1 (red). (D) Significantly higher values of TuJ1 expression were observed in cochlear nonsensory epithelial cells transfected with *Ascl.nucEGFP* than those transfected with a *pCIG.EGFP* control vector. No TuJ1-positive cells were induced in cells at E13.5 electroporated with a *pCIG.EGFP* control vector. The efficiency of neuron induction by Ascl1 remained consistently high up to P10, with no significant differences among ages. (E) Significantly higher values of TuJ1 expression were observed in cochlear sensory epithelial cells transfected with *Ascl.nucEGFP* than those transfected with a *pCIG.EGFP* control vector. No TuJ1-positive cells were induced in sensory epithelial cells at E13.5 electroporated with a *pCIG.EGFP* control vector. There was no difference of the efficiency of neuron induction by Ascl1 between E13.5 and P20. Scale bar: A (for A–C), 20 μm. (For interpretation of the references to color in this figure legend, the reader is referred to the web version of this article.)

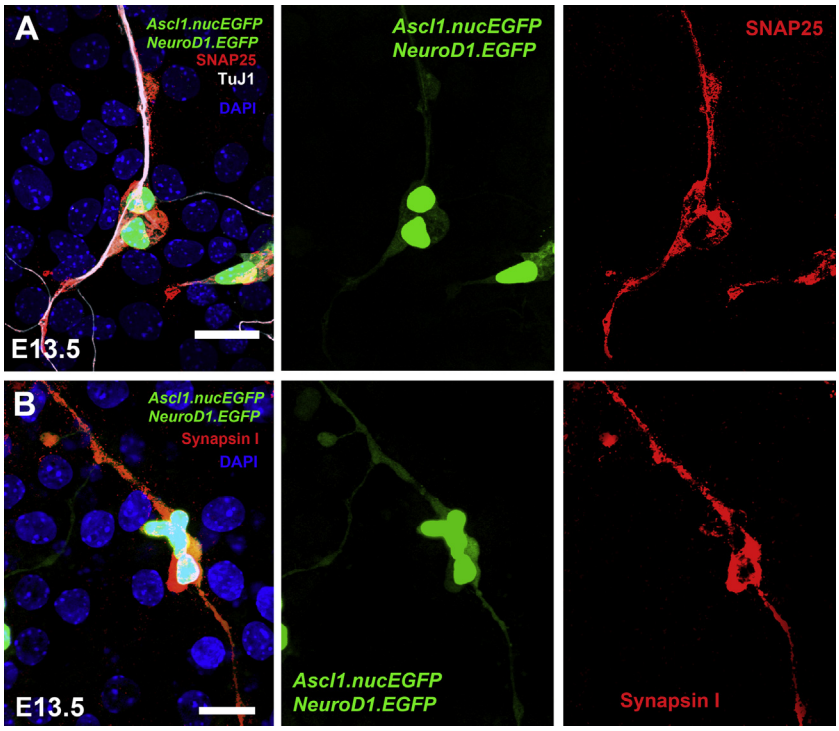

Fig. 4. Ascl1- and NeuroD1-induced synaptic proteins. High-magnification images of E13.5 cochlear non-sensory epithelial cells electroporated with *Ascl1.nucEGFP* and *NeuroD1.EGFP* (green) maintained for 6 DIV showing the expression of synaptic proteins. Merged views are shown on the left (A, B) and individual channels are to the right. Doubly transfected cells expressed SNAP25 (A in red) with TuJ1 (A in white)-positive neurites. Doubly transfected cells also expressed SynapsinI (B in red). Scale bars: A and B, 20 μm. (For interpretation of the references to color in this figure legend, the reader is referred to the web version of this article.)

To investigate whether the overexpression of *Ascl1* in cochlear epithelial cells induces membrane properties resembling those of endogenous ANs, we compared electrophysiological recordings of *pCIG-Ascl1*-transfected cells and control recordings made from cells transfected with pCIG empty vector. A total number of 13 control recordings consistently showed limited or no voltage-dependent whole-cell currents (n = 8; Fig. 5B) under voltage clamp configuration. This observation was substantiated by ohmic responses observed in current clamp mode (Fig. 5C), which are consistent with passive membrane properties. In contrast, Ascl1-transfected cells exhibited significant voltage-dependent whole-cell conductances (Fig. 5E, F). All recorded cells exhibited voltage-dependent outward currents and 16 out of a total of 22 recordings (72.7%, Table 1) showed inactivating inward currents characteristic of an excitable cell. Whole-cell conductance measurements could be measured from a subset of the recordings and revealed an average inward conductance of 3.8 ± 0.8 nS (n = 9) and average outward conductance of 17.6 ± 2.3 nS (n = 14) and 9.3 ± 1.8 nS at the peak and plateau, respectively. Moreover, action potential profiles were observed in Ascl1-transfected cells in current clamp mode (Fig. 5G). Action potentials (n = 5) in the *Ascl1*-transfected cells showed longer overall latency (50.0 ± 10.8 ms) and duration (7.7 ± 2.1 ms) than endogenous postnatal ANs (Adamson et al., 2002; Latency: 14.2 ± 0.7 ms in the base, 31.1 ± 3.0 ms in the apex; duration: 1.7 ± 0.1 ms in the base, 2.2 ± 0.2 ms in the apex).

Our previous data suggested that NeuroD1 was sufficient to reprogram cochlear non-sensory epithelial cells into neuronal morphology (Puligilla et al., 2010). To examine whether NeuroD1 overexpression would also induce neuronal membrane properties, we recorded from cochlear epithelial cells transfected with a *pCLIG-NeuroD1* vector. Nine out of 12 recordings showed voltage-dependent whole-cell currents; while eight cells exhibited different levels of outward currents, only two cells displayed a slow, low-amplitude inward current (Table 1). Whole-cell conductance measurements were made when possible and revealed average whole-cell outward conductance of 13.6 ± 6.4 nS (n = 5) and 6.8 ± 4.0 nS (n = 5) at the peak and plateau, respectively. Both fast-inactivating and slow-inactivating kinetics of the outward currents were observed (Fig. 5H-K). Overall, unlike *Ascl1*, overexpression of *NeuroD1* alone was not able to induce neuronal-like membrane properties in cochlear epithelial cells.

It was recently reported that the overexpression of *NeuroD1* alone in human fibroblasts did not have a notable effect; however, its combination with other factors significantly improved the efficiency of neuron induction (Pang et al., 2011). Therefore we asked whether the combination of *NeuroD1* with *Ascl1* could improve the induction of neuron-like membrane properties in cochlear epithelial cells. Whereas slightly lower percentage of *Ascl1-NeuroD1* double-transfected cells (57.7%, Table 1) showed inward currents (Fig. 5L) compared to those transfected with *Ascl1* only, the average

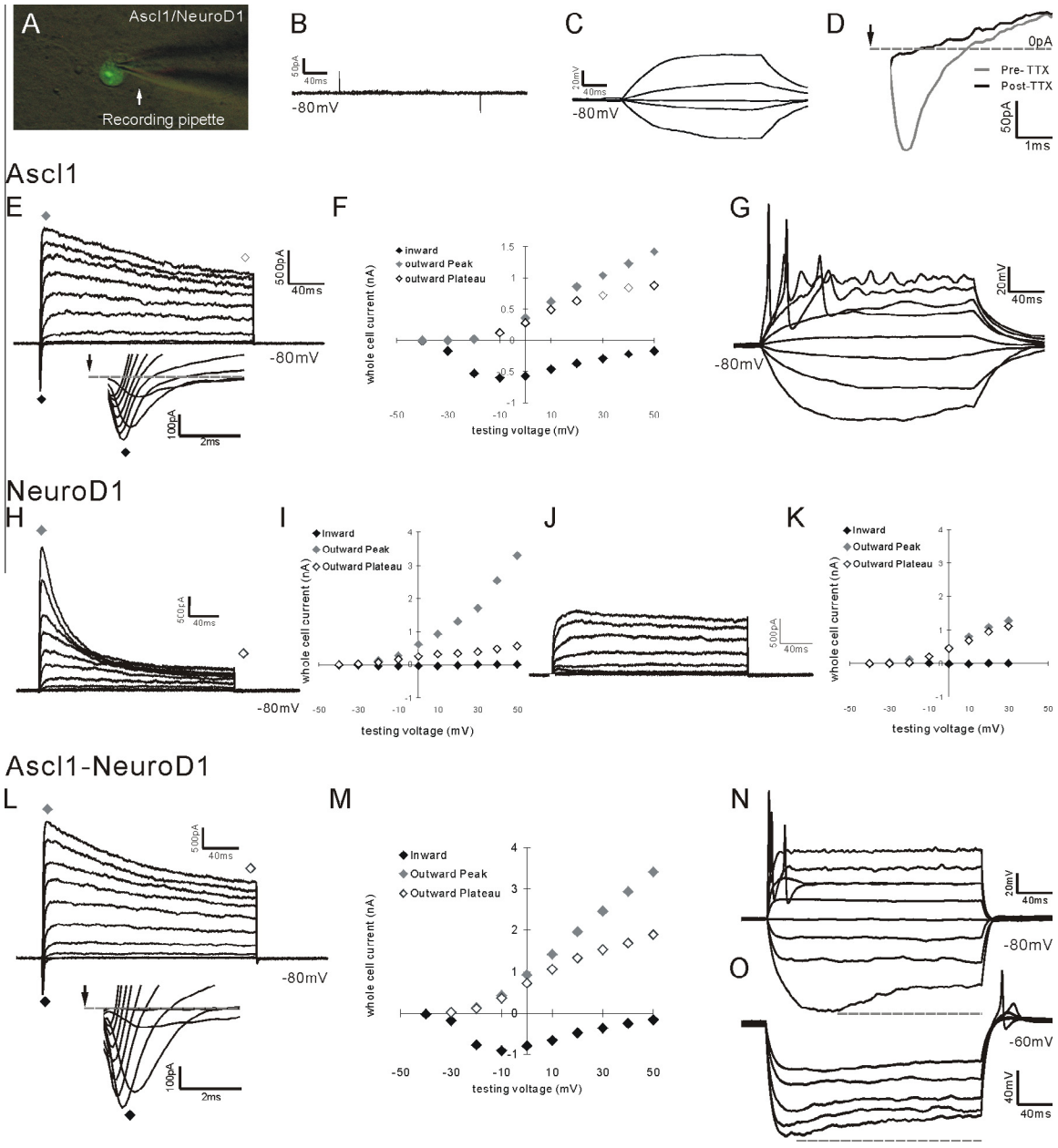

Fig. 5. Induction of neuronal-like electrophysiological features in E13.5 cochlear non-sensory epithelial cells. Dissociated E13.5 cochlear epithelial cells overexpressing Ascl1, Ascl1 and NeuroD1 or empty vector were recorded on DIV 3–8. (A) A merged image of Hoffman contrast and green fluorescence shows a recording pipette attached to a GFP-positive cell. (B, C) A cell transfected with empty vector showed very limited whole-cell currents (B) when depolarized with steps of −30 to 50 mV from −80 mV holding potential under voltage clamp and exhibited ohmic passive membrane responses (C) to current injections of −4 to 4 pA at −80 mV holding potential under current clamp. (D) Inactivating inward currents (with depolarization to −10 mV from −80 mV holding potential) induced by Ascl1–NeuroD1 transfection could be completely abolished by 1 μM TTX. Gray, before drug application; black, after drug application. (E–G) Ascl1 transfection induced a neuronal-like phenotype on DIV 4. (E) An Ascl1-transfected cell showed both voltage-dependent whole-cell outward currents and inactivating whole-cell inward currents (black diamond) when depolarized with steps of −40 to 50 mV from -80 mV holding potential. Inset, A high magnification view of the inward currents in E. (F) Whole-cell voltage–current relation of the recording shown in E. The peak (gray diamond) and plateau (open diamond) of outward currents were measured at different positions of the traces as indicated in E. (G) Immature action potentials were revealed in current clamp recording from the same cell as in E and F with currents ranging from −3 to 22 pA. (H–K) NeuroD1 transfection induced different types of outward currents but no fast inactivating inward currents as observed in E. H, Recording from a NeuroD1-transfected cell on DIV4 showed large inactivating outward currents but no inward currents in response to depolarization from −40 to 50 mV. I, current–voltage relation of the recording in H. J, Another example of a recording from a NeuroD1-transfected cell that displayed slowly inactivating outward currents under voltage steps from −40 to +30 mV. (K) Current–voltage relation of the recording in J. (L–N) Recordings from Ascl1-NeuroD1 double transfected on DIV 8. L, voltage clamp traces exhibiting large inward and outward whole-cell current when depolarized with steps of −40 to 50 mV. Inset, inactivating inward currents shown in a high magnification. (M) Whole-cell voltage–current relation of the recording shown in L. (N) Whole-cell current clamp recordings from the same cell. Currents ranging from −65 to 420 pA were injected. (O) A rebound spike was observed in an exemplifying current clamp recording from another Ascl1-NeuroD1 double-transfected cell, which was held at −60 mV and hyperpolarized by −60 to −190 pA current injection. Dashed lines in N and O indicate hyperpolarizing sag. In panels D, E inset and L inset, arrow indicates the onset of stimulus and initial portion of the traces with capacitive transients were removed.

Table 1. Ascl1 overexpression induces inward conductance in E13.5 cochlear epithelial cells

Transfection	pCIG vector	Ascl1	NeuroD1	Ascl1-NeuroD1
Total No. of recordings	13	22	12	26
Percentage of cells with inward current	0	72.7% (16)	16.7% (2)	57.7% (15)
Inward conductance (nS)	–	3.8 ± 0.8 (n = 9)	1.8 ± 0.6 (n = 2)	4.3 ± 1.0 (n = 11)
Percentage of cells with outward current	61.5% (8)	100%	75% (8)	100%
Peak outward conductance (nS)	0.4 ± 0.2 (n = 4)	17.6 ± 2.3 (n = 14)	13.6 ± 6.4 (n = 5)	22.7 ± 3.9 (n = 19)

inward whole-cell conductance (4.3 ± 1.0 nS, n = 11) and average outward conductance at peak (22.7 ± 3.9 nS, n = 19) and plateau (15.7 ± 3.3 nS, n = 19) in the double-transfected cells showed a slight trend toward larger conductances but were not significantly different ($p > 0.10$). Action potential profile of the Ascl1-NeuroD1 double-transfected cells (latency: 52.9 ± 14.4 ms; duration: 5.1 ± 1.9 ms; n = 4; Fig. 5M) was comparable to that of the Ascl1-transfected cells described above. Inward currents could be abolished by the application of TTX (Fig. 5D), suggesting that a robust Na^+ current contributes to the action potential profiles observed in whole-cell current clamp recordings (Fig. 5D). Furthermore, in both Ascl1 and Ascl1-NeuroD1-transfected cells there were clear indications of hyperpolarization-induced voltage sag and, in an example with double transfection, (Fig. 5O) rebound action potentials were also observed. Both results are suggestive of the presence of I_h, which were also reported in ANs (Chen, 1997; Mo and Davis, 1997; Liu and Davis, 2007).

DISCUSSION

We have utilized a neurogenic transcription factor to induce at high efficiency an endogenous population of cochlear non-sensory epithelial cells into becoming functioning neurons at embryonic, postnatal and juvenile stages. This is a first step in replacing lost or damaged ANs that might lead to the amelioration of hearing loss.

The bHLH neurogenic transcription factor *Ascl1* is homologous to proneural genes in *Drosophila* (Johnson et al., 1990), expressed in the developing nervous systems (Kageyama et al., 1997) and required for the early development of olfactory and autonomic neurons (Guillemot et al., 1993). Results of this study demonstrate that *Ascl1* induces functional neurons directly from cochlear non-sensory epithelial cells that would not normally develop as neurons, concurring with the report that *Ascl1* alone was sufficient to induce neurons from mouse fibroblasts (Vierbuchen et al., 2010). Moreover, the vast majority of induced neurons became post mitotic 24 h after transgene activation, suggesting *Ascl1* is a reprogramming factor that promotes neuronal differentiation without proliferation (Vierbuchen et al., 2010). Thus, stochastic nature of transfection accompanied with electroporation, not proliferation, may result in patches of induced neurons in the present study (Fig. 2B, C). Our current results support our previous finding that otocyst-derived nonsensory epithelial cells initially maintain their neurogenic capacity (Puligilla et al., 2010), and given the right factor(s), their competency extends beyond embryonic stages.

The high efficiency of neuron induction by *Ascl1* in combination with its ability to induce neurons at juvenile stages has significant implications for induction and regeneration of neurons in the adult cochlea for the purposes of therapy and repair for hearing loss. In humans, sensorineural hearing loss is the primary type of congenital and acquired hearing loss. Several studies have shown that in animals, a secondary effect of loss of hair cells after damage to the inner ear from ototoxic medication, aging and or acoustic trauma is loss of ANs (Miller, 2001). However, more recently it has been shown that loss of ANs is a primary and direct effect of noise-induced damage. This primary loss of ANs is likely the main contributing factor to difficulties experienced when trying to hear in noisy environments (Kujawa and Liberman, 2009; Lin et al., 2011; Furman et al., 2013). ANs in the cochlea play a critical role in hearing, as they are the primary afferent neurons that transmit auditory information from mechanosensory hair cells in the inner ear to the brain. Current amplification strategies depend on the existence of even a few functioning neurons (Linthicum and Anderson, 1991; Khan et al., 1998). Thus, the ability to successfully induce neurons from existing cells from the cochlea could have a significant impact on research and advancement in cochlear implants as well as in the medical treatment of hearing loss and deafness.

One approach to replace lost ANs is cell transplantation. Induced pluripotent stem cell-derived neural progenitors have the potential to replace ANs *in vivo* (Nishimura et al., 2009, 2012). More recently, a report has shown that human embryonic stem-cell-derived otic neuroprogenitors transplanted into the modiolus partially restored auditory brainstem responses (Chen et al., 2012). However, other reports point to the dangers of introducing exogenous stem cells (Miura et al., 2009; Nishimura et al., 2012). An alternative method to replace lost ANs is to induce a phenotypic transdifferentiation of non-neural cells that remain in the deaf cochlea to neurons. While several researchers evaluated a protective effect of neurotrophins on ANs by gene therapy (Shibata et al., 2009; Wise et al., 2011; Wu et al., 2011), there are no reports at this time on inducing endogenous ANs in the adult by gene transduction. Our *ex vivo* study to evaluate neural competence of cochlear non-sensory epithelial cells at the juvenile stage is a first step to induce endogenous ANs *in vivo* and later examine functional regeneration. Generation of induced neurons via direct conversion *in vivo* (Torper et al., 2013) suggests the feasibility of inducing ANs *in vivo*.

Our results demonstrated several similarities between the induced neurons and endogenous ANs in neuronal

protein expression: In addition to TuJ1, Map2 is also expressed in induced neurons (Fig. 2C) and in the body and central processes of maturing ANs (Hafidi et al., 1992); Prox1 induction in nonsensory epithelial cells (Fig. 2D) is similar to endogenous ANs (Bermingham-McDonogh et al., 2006). Induced neurons expressed SNAP25 (Fig. 4A), consistent with the previous report that low-frequency ANs showed high SNAP25 protein levels (Flores-Otero and Davis, 2011). An *in vitro* culture may alter the distribution of presynaptic SNAP25 and Synapsin I at cell bodies and the neuron extensions of induced neurons, as cocultures of primary AN explants and auditory epithelia found that the processes from ANs express markers for presynaptic fibers (Martinez-Monedero et al., 2006). Another possibility is presynaptic proteins of induced neurons are under transportation to the nerve terminal.

Not only neuronal induction but also differentiation, maturation and survival are essential for functioning induced neurons. To achieve this goal, we used another bHLH transcription factor, *NeuroD1*. *NeuroD1*-null mice show failure of survival of SGNs during development due to lack of neurotrophin receptors, TrkB and TrkC, suggesting *NeuroD1* plays a role in neuronal differentiation, survival and target selection of peripheral projections (Kim et al., 2001), because TrkB-null mice reduced innervation of the outer hair cells in the apical and middle turns of the cochlea and TrkC-null mice lose many ANs predominantly in the basal turn of the cochlea (Fritzsch et al., 1998). Unexpectedly, there is no significant difference regarding synaptic protein expression, their distribution and electrophysiological properties between *Ascl1*-induced neurons and *Ascl1*- and *NeuroD1*-induced neurons, suggesting additional cues are needed for inducing maturations.

In summary, we found that with either *Ascl1* single or *Ascl1-NeuroD1* double overexpression, action potentials were unequivocally induced in cochlear epithelial cells. Interestingly, more than 30% (three out of the nine) of all available current clamp recordings showed action potential latency comparable to early postnatal ANs, the average latency of which was 14.8 ± 1.5 ms in the base and 30.7 ± 2.8 ms in the apex (Adamson et al., 2002), the remaining transfected cells had prolonged latencies that exceeded these levels. Furthermore, although 8 recordings showed prolonged action potential duration compared to postnatal ANs, one cell exhibited brief action potential duration that matched the profile of an average basal neuron (Fig. 5N). These observations suggested that the overexpression of *Ascl1* and *NeuroD1* can induce excitable membrane properties that in some cases closely resemble the fast firing kinetics of ANs. To evaluate this more closely we compared the action potentials parameters and whole-cell conductances from eight recordings transfected with either *Ascl1* alone or in combination with *NeuroD1*, and found that those with the largest whole-cell peak outward conductances displayed firing parameters with the fastest latency (least squares linear regression, $R^2 = 0.81$), and those with the largest inward conductance possessed the greatest action potential amplitudes ($R^2 = 0.45$). We, therefore, expect that with larger whole-cell inward and outward conductances, the electrophysiological profile of the induced neuronal-like cells may progressively resemble that of mature ANs. Moreover, we also observed recordings with a prominent hyperpolarizing sag suggesting that these induced neuronal-like cells may also possess I_h currents that play important roles in the regulation of firing threshold in endogenous postnatal neurons (Liu et al., 2014).

ANs must not only express neuronal proteins and have neuronal morphology, but also fire action potentials, express synaptic proteins, and make contact and communicate with cochlear hair cells in the periphery and cochlear nuclei neurons in the brainstem. Further studies are needed to test the feasibility of induced neurons to make synaptic contacts with cochlear hair cells in the periphery and cochlear nuclei neurons centrally.

AUTHOR CONTRIBUTIONS

K.N., R.M.W., W.L. R.D and A.D., designed research; K.N., R.M.W. and W.L. performed research; K.N., R.M.W., W.L., and A.D, analyzed data; and K.N, R.M.W., W.L. R.D. and A.D. wrote the paper.

FINANCIAL SUPPORT

This work was supported by the Shulsky Foundation (A.D.) and the Capita Foundation (A.D.); the Kyoto University Foundation (K.N.) and Sumitomo Life Social Welfare Services Foundation (K.N.); NIH NIDCD R01-DC01856 (R.D.); and the Hearing Regeneration Initiative at Sunnybrook.

Acknowledgments—The authors would like to thank Dr. S. Pons from the Institute for Biomedical Research of Barcelona, Barcelona, Spain, for generously providing the Ascl1 expression plasmid, Willy Sun for technical assistance and Drs. S. Heller, I. Aubert and A.J. Matsuoka for commenting on an earlier version of the manuscript.

REFERENCES

Adamson CL, Reid MA, Mo ZL, Bowne-English J, Davis RL (2002) Firing features and potassium channel content of murine spiral ganglion neurons vary with cochlear location. J Comp Neurol 447:331–350.

Alvarez-Rodriguez R, Pons S (2009) Expression of the proneural gene encoding Mash1 suppresses MYCN mitotic activity. J Cell Sci 122:595–599.

Bahmad Jr F, Merchant SN, Nadol Jr JB, Tranebjaerg L (2007) Otopathology in Mohr–Tranebjaerg syndrome. Laryngoscope 117:1202–1208.

Bermingham-McDonogh O, Oesterle EC, Stone JS, Hume CR, Huynh HM, Hayashi T (2006) Expression of Prox1 during mouse cochlear development. J Comp Neurol 496:172–186.

Castro DS, Martynoga B, Parras C, Ramesh V, Pacary E, Johnston C, Drechsel D, Lebel-Potter M, Garcia LG, Hunt C, Dolle D, Bithell A, Ettwiller L, Buckley N, Guillemot F (2011) A novel function of the proneural factor Ascl1 in progenitor proliferation identified by genome-wide characterization of its targets. Genes Dev 25:930–945.

Chen C (1997) Hyperpolarization-activated current (Ih) in primary auditory neurons. Hear Res 110:179–190.

Chen W, Jongkamonwiwat N, Abbas L, Eshtan SJ, Johnson SL, Kuhn S, Milo M, Thurlow JK, Andrews PW, Marcotti W, Moore HD, Rivolta MN (2012) Restoration of auditory evoked responses by human ES-cell-derived otic progenitors. Nature 490:278–282.

Dabdoub A, Puligilla C, Jones JM, Fritzsch B, Cheah KS, Pevny LH, Kelley MW (2008) Sox2 signaling in prosensory domain specification and subsequent hair cell differentiation in the developing cochlea. Proc Natl Acad Sci U S A 105:18396–18401.

Davis RL, Weintraub H, Lassar AB (1987) Expression of a single transfected cDNA converts fibroblasts to myoblasts. Cell 51:987–1000.

De Camilli P, Cameron R, Greengard P (1983) Synapsin I (protein I), a nerve terminal-specific phosphoprotein. I. Its general distribution in synapses of the central and peripheral nervous system demonstrated by immunofluorescence in frozen and plastic sections. J Cell Biol 96:1337–1354.

Engle JR, Tinling S, Recanzone GH (2013) Age-related hearing loss in rhesus monkeys is correlated with cochlear histopathologies. PLoS One 8:e55092.

Flores-Otero J, Davis RL (2011) Synaptic proteins are tonotopically graded in postnatal and adult type I and type II spiral ganglion neurons. J Comp Neurol 519:1455–1475.

Flores-Otero J, Xue HZ, Davis RL (2007) Reciprocal regulation of presynaptic and postsynaptic proteins in bipolar spiral ganglion neurons by neurotrophins. J Neurosci 27:14023–14034.

Fritzsch B, Barbacid M, Silos-Santiago I (1998) The combined effects of trkB and trkC mutations on the innervation of the inner ear. Int J Dev Neurosci 16:493–505.

Furman AC, Kujawa SG, Liberman MC (2013) Noise-induced cochlear neuropathy is selective for fibers with low spontaneous rates. J Neurophysiol 110:577–586.

Gu G, Dubauskaite J, Melton DA (2002) Direct evidence for the pancreatic lineage: NGN3+ cells are islet progenitors and are distinct from duct progenitors. Development 129:2447–2457.

Guillemot F, Lo LC, Johnson JE, Auerbach A, Anderson DJ, Joyner AL (1993) Mammalian achaete-scute homolog 1 is required for the early development of olfactory and autonomic neurons. Cell 75:463–476.

Hafidi A, Fellous A, Ferhat L, Romand MR, Romand R (1992) Developmental differentiation of MAP2 expression in the central versus the peripheral and efferent projections of the inner ear. J Comp Neurol 323:423–431.

Hallworth R, McCoy M, Polan-Curtain J (2000) Tubulin expression in the developing and adult gerbil organ of Corti. Hear Res 139:31–41.

Inoue T, Hojo M, Bessho Y, Tano Y, Lee JE, Kageyama R (2002) Math3 and NeuroD regulate amacrine cell fate specification in the retina. Development 129:831–842.

Johnson JE, Birren SJ, Anderson DJ (1990) Two rat homologues of Drosophila achaete-scute specifically expressed in neuronal precursors. Nature 346:858–861.

Jones JM, Montcouquiol M, Dabdoub A, Woods C, Kelley MW (2006) Inhibitors of differentiation and DNA binding (Ids) regulate Math1 and hair cell formation during the development of the organ of Corti. J Neurosci 26:550–558.

Kageyama R, Ishibashi M, Takebayashi K, Tomita K (1997) BHLH transcription factors and mammalian neuronal differentiation. Int J Biochem Cell Biol 29:1389–1399.

Karalay O, Doberauer K, Vadodaria KC, Knobloch M, Berti L, Miquelajauregui A, Schwark M, Jagasia R, Taketo MM, Tarabykin V, Lie DC, Jessberger S (2011) Prospero-related homeobox 1 gene (Prox1) is regulated by canonical Wnt signaling and has a stage-specific role in adult hippocampal neurogenesis. Proc Natl Acad Sci U S A 108:5807–5812.

Khan ZH, Mohapatra SK, Khodiar PK, Ragu Kumar SN (1998) Artificial neural network and medicine. Indian J Physiol Pharmacol 42:321–342.

Kim WY, Fritzsch B, Serls A, Bakel LA, Huang EJ, Reichardt LF, Barth DS, Lee JE (2001) NeuroD-null mice are deaf due to a severe loss of the inner ear sensory neurons during development. Development 128:417–426.

Kujawa SG, Liberman MC (2009) Adding insult to injury: cochlear nerve degeneration after "temporary" noise-induced hearing loss. J Neurosci 29:14077–14085.

Lee MK, Rebhun LI, Frankfurter A (1990) Posttranslational modification of class III beta-tubulin. Proc Natl Acad Sci U S A 87:7195–7199.

Lin HW, Furman AC, Kujawa SG, Liberman MC (2011) Primary neural degeneration in the Guinea pig cochlea after reversible noise-induced threshold shift. J Assoc Res Otolaryngol JARO 12:605–616.

Linthicum Jr FH, Anderson W (1991) Cochlear implantation of totally deaf ears. Histol Eval Candidacy Acta Oto-Laryngol 111:327–331.

Liu Q, Davis RL (2007) Regional specification of threshold sensitivity and response time in CBA/CaJ mouse spiral ganglion neurons. J Neurophysiol 98:2215–2222.

Liu Q, Lee E, Davis RL (2014) Heterogeneous intrinsic excitability of murine spiral ganglion neurons is determined by Kv1 and HCN channels. Neuroscience 257:96–110.

Makary CA, Shin J, Kujawa SG, Liberman MC, Merchant SN (2011) Age-related primary cochlear neuronal degeneration in human temporal bones. J Assoc Res Otolaryngol JARO 12:711–717.

Martinez-Monedero R, Corrales CE, Cuajungco MP, Heller S, Edge AS (2006) Reinnervation of hair cells by auditory neurons after selective removal of spiral ganglion neurons. J Neurobiol 66:319–331.

Masuda M, Pak K, Chavez E, Ryan AF (2012) TFE2 and GATA3 enhance induction of POU4F3 and myosin VIIa positive cells in nonsensory cochlear epithelium by ATOH1. Dev Biol 372:68–80.

Miller AL (2001) Effects of chronic stimulation on auditory nerve survival in ototoxically deafened animals. Hear Res 151:1–14.

Miura K, Okada Y, Aoi T, Okada A, Takahashi K, Okita K, Nakagawa M, Koyanagi M, Tanabe K, Ohnuki M, Ogawa D, Ikeda E, Okano H, Yamanaka S (2009) Variation in the safety of induced pluripotent stem cell lines. Nat Biotechnol 27:743–745.

Mo ZL, Davis RL (1997) Heterogeneous voltage dependence of inward rectifier currents in spiral ganglion neurons. J Neurophysiol 78:3019–3027.

Nadol Jr JB, Merchant SN (2001) Histopathology and molecular genetics of hearing loss in the human. Int J Pediatr Otorhinolaryngol 61:1–15.

Nishimura K, Nakagawa T, Ono K, Ogita H, Sakamoto T, Yamamoto N, Okita K, Yamanaka S, Ito J (2009) Transplantation of mouse induced pluripotent stem cells into the cochlea. NeuroReport 20:1250–1254.

Nishimura K, Nakagawa T, Sakamoto T, Ito J (2012) Fates of murine pluripotent stem cell-derived neural progenitors following transplantation into mouse cochleae. Cell Transplant 21:763–771.

Ono K, Nakagawa T, Kojima K, Matsumoto M, Kawauchi T, Hoshino M, Ito J (2009) Silencing p27 reverses post-mitotic state of supporting cells in neonatal mouse cochleae. Mol Cell Neurosci 42:391–398.

Pang ZP, Yang N, Vierbuchen T, Ostermeier A, Fuentes DR, Yang TQ, Citri A, Sebastiano V, Marro S, Sudhof TC, Wernig M (2011) Induction of human neuronal cells by defined transcription factors. Nature 476:220–223.

Puligilla C, Dabdoub A, Brenowitz SD, Kelley MW (2010) Sox2 induces neuronal formation in the developing mammalian cochlea. J Neurosci 30:714–722.

Rizo J, Sudhof TC (2002) Snares and Munc18 in synaptic vesicle fusion. Nat Rev Neurosci 3:641–653.

Rubel EW, Fritzsch B (2002) Auditory system development: primary auditory neurons and their targets. AnnuQ Rev Neurosci 25:51–101.

Sergeyenko Y, Lall K, Liberman MC, Kujawa SG (2013) Age-related cochlear synaptopathy: an early-onset contributor to auditory functional decline. J Neurosci 33:13686–13694.

Shibata SB, Di Pasquale G, Cortez SR, Chiorini JA, Raphael Y (2009) Gene transfer using bovine adeno-associated virus in the guinea pig cochlea. Gene Ther 16:990–997.

Shupliakov O, Haucke V, Pechstein A (2011) How synapsin I may cluster synaptic vesicles. Semin Cell Dev Biol 22:393–399.

Takahashi K, Merchant SN, Miyazawa T, Yamaguchi T, McKenna MJ, Kouda H, Iino Y, Someya T, Tamagawa Y, Takiyama Y, Nakano I, Saito K, Boyer P, Kitamura K (2003) Temporal bone histopathological and quantitative analysis of mitochondrial DNA in MELAS. Laryngoscope 113:1362–1368.

Torper O, Pfisterer U, Wolf DA, Pereira M, Lau S, Jakobsson J, Bjorklund A, Grealish S, Parmar M (2013) Generation of induced neurons via direct conversion in vivo. Proc Natl Acad Sci U S A 110:7038–7043.

Vierbuchen T, Ostermeier A, Pang ZP, Kokubu Y, Sudhof TC, Wernig M (2010) Direct conversion of fibroblasts to functional neurons by defined factors. Nature 463:1035–1041.

Wise AK, Tu T, Atkinson PJ, Flynn BO, Sgro BE, Hume C, O'Leary SJ, Shepherd RK, Richardson RT (2011) The effect of deafness duration on neurotrophin gene therapy for spiral ganglion neuron protection. Hear Res 278:69–76.

Wu J, Liu B, Fan J, Zhu Q, Wu J (2011) Study of protective effect on rat cochlear spiral ganglion after blast exposure by adenovirus-mediated human beta-nerve growth factor gene. Am J Otolaryngol 32:8–12.

Zhou Q, Brown J, Kanarek A, Rajagopal J, Melton DA (2008) In vivo reprogramming of adult pancreatic exocrine cells to beta-cells. Nature 455:627–632.

(Accepted 14 May 2014)
(Available online 11 June 2014)